Performance Analysis in the Downlink of Asynchronous OFDM/FBMC Based Multi-Cellular Networks

Yahia Medjahdi, Michel Terré, Didier Le Ruyet, *Member, IEEE,* Daniel Roviras, and Ali Dziri, *Member, IEEE*

Abstract—This paper provides a theoretical performance evaluation of the downlink of asynchronous orthogonal frequency division multiplexing (OFDM) and filter bank based multicarrier (FBMC) cellular radio communication systems. An accurate derivation, for the interference caused by the timing synchronization errors in the neighboring cells, is developed. The multipath effects on the interfering and desired signal are also considered. Based on computing the moment generating functions of the interference power, exact expressions are derived for average error rates of OFDM and FBMC systems considering the frequency correlation fading in the case of block subcarrier assignment scheme.

Index Terms—Inter-channel interference, OFDM, FBMC, asynchronous, frequency selective channel, moment generating function (MGF), correlated Rayleigh fading.

I. INTRODUCTION

BEYOND traditional voice communication, wireless networks are currently evolving to support high speed data applications such as video streaming and internet browsing [1]. However, wireless communication systems are subject to several impairments such as fading, pathloss and interference. These effects can seriously degrade the quality of service and lead to transmission failures.

An orthogonal Frequency Division Multiplexing (OFDM) system is a type of multicarrier modulation which consists of splitting up a wide band signal at a high symbol rate into several lower rate signals, each one occupying a narrower band. System performance improves because subcarriers experience flat fading channels and are orthogonal to one another thus minimizing the threat of interference. However, the OFDM performance tends to suffer from degradation because of possible episodes of imperfect time and frequency synchronization, since a loss in orthogonality can occur between subcarriers at the OFDM receiver [2].

The impact of asynchronous interference in OFDM systems has been intensively investigated in the literature. A performance analysis of OFDM in the presence of timing synchronization can be found in [2], [3], [4], [5]. Using the Gaussian approximation for interchannel interference, [6] gives approximate expressions of the symbol error rates. Moreover, the degradation of the signal to interference plus noise ratio is a common criterion to analyze the impact of timing non-synchronization on the system performance [3], [7]. In [5], an interference modeling based on the so called Interference Table [4], has been developed for two multicarrier techniques: CP-OFDM with a rectangular pulse shape and for Filter Bank based Multi-Carrier (FBMC) with a prototype filter designed for a better frequency selectivity using the frequency sampling technique [8].

Although interference analysis in OFDM single user has become popular in literature e.g [9], [10], [11], the extension of this analysis to a multi-cellular environment is not so straightforward. This problem is significant for the following reasons. First, in a multi-cellular environment the interference stems from subcarriers distributed among several transmitters which require more than one random variable (RV) to model this interference, therefore, the analysis becomes more difficult. Second, in contrast to many researches based on the classical Gaussian approximation [6], [12], we cannot always rely on this approximation. For example, when the number of interferers is large but there are dominant interferers, the central limit theorem is no longer applicable [13], [14].

This paper presents an analytical interference analysis related to asynchronous downlink OFDM/FBMC in multicellular environment, providing exact expressions of average error rates in frequency selective fading channels.

The evaluation of the average error rate of a given transmission is considered as the most common criterion used in the investigation of the impact of interference on the system performance. Beaulieu [15], [16], based on the Fourier series and a Chernoff bound technique, was able to express the average of the Gaussian complementary distribution function. A recent study [2] has presented a theoretical analysis of the average error rate of an asynchronous OFDM system in the special case of interleaved subcarrier assignment scheme. However, to the best of our knowledge, there is no paper addressing the impact of the asynchronous interference on the bit error rate of the FBMC systems. Based on the interference table model introduced in [5], we derive in this paper an explicit expression of the bit error rate of time-asynchronous OFDM and FBMC systems in the case of the block subcarrier assignment, taking into account the correlation between the subchannel gains belonging to a given block subcarrier. The
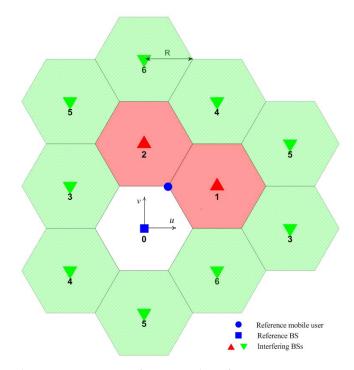
Fig. 1: The geometry of the downlink of OFDM/FBMC based networks with a cluster size of 7.

computation of the average error rate is based on the moment generating function of the interference power.

The outline of this paper is organized as follows. Section II is devoted to describing the system model of the downlink of OFDM and FBMC based multi-cellular networks. A brief review of interference table modeling is given in Section III. We further derive explicit expressions of the average error rates of asynchronous OFDM/FBMC systems in Section IV. Simulation results are presented and discussed in Section V. Section VI provides a summary and a discussion of some extensions of the paper.

II. THE SYSTEM MODEL

We consider the downlink transmission in OFDM/FBMC based multi-cellular networks depicted in Fig. 1. The reference mobile user is located at (u, v). The reference base station is assumed to be situated at the origin $(u_0, v_0) = (0, 0)$. In this analysis, we consider two tiers of the neighboring cells that are surrounding the reference mobile user. Let the k-th base station be located at (u_k, v_k), then, the distance between the reference mobile user and the k-th base station is given by

$$d_k = \sqrt{(u_k - u)^2 + (v_k - v)^2} \qquad (1)$$

The cell radius is denoted by R in Fig. 1.

Concerning the frequency reuse scheme, the subcarriers are allocated according to the most common subcarrier assignment scheme, namely, the block subcarrier assignment scheme [2] which is described in Fig. 2. We assume in this scheme that δ adjacent subcarriers to each block are free and serve as guard bands between the different blocks.

All signals propagate through different multipath channels using a similar propagation model, where the impulse response
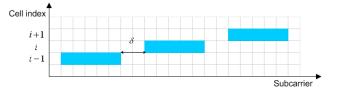

Fig. 2: Block subcarrier assignment scheme with $\delta = 2$.

of the multipath channel between the k-th base station and the reference mobile user is given by

$$h_k(t) = \sum_{i=0}^{L-1} h_{k,i} \delta(t - \frac{n_{k,i}}{N} T) \qquad (2)$$

where $n_{k,0} < n_{k,1} < ... < n_{k,(L-1)} < C$ and C is the maximum delay spread of the channel normalized by the sampling period (T/N), and $h_{k,i}$ are the complex channel path gains, which are assumed mutually independent, where $\mathbb{E}[h_{k,i} h_{k,i}^*] = \gamma_{k,i}$, and $\mathbb{E}[h_{k,i} h_{k,j}^*] = 0$ when $i \neq j$. We further assume that the power is normalized for each channel such that $\sum_{i=0}^{L-1} \gamma_{k,i} = 1, \forall k$. T and N denote respectively the OFDM symbol duration and the total number of subcarriers in the system.

We also assume that the propagation channels are stationary over one OFDM symbol. This is the case for time-invariant or slowly varying channels. Furthermore, the underlying channel model includes path-loss effects which take into account the positions of the base stations with respect to the reference mobile user.

The reference mobile user is assumed to be perfectly synchronized with its base station but it is not necessarily synchronized with the other base stations. We can express the composite signal at the reference receiver by the sum of the desired signal coming from the reference base station and the interference signal coming from the surrounding base stations,

$$r(t) = \underbrace{d_0^{-\beta/2} s_0(t) * h_0(t)}_{\text{desired signal}}$$
$$+ \underbrace{\sum_{k=1}^{K} d_k^{-\beta/2} s_k(t - \tau_k) * h_k(t)}_{\text{interference signal}} + n(t) \qquad (3)$$

where

- K is the total number of neighboring cells
- $s_k(t)$ is the transmitted signal from the k-th base station
- τ_k denotes the timing offset between the reference mobile user and the k-th base station
- $n(t)$ is the additive white Gaussian noise (AWGN)
- β is the path loss exponent

Because of the timing misalignment between the neighboring cells and the reference one, the signals arriving from the cells in the vicinity will appear non-orthogonal to the desired signal. This non-orthogonality will generate interference and will degrade the SINR. This degradation will be investigated in the next section.

III. INTERFERENCE AND SINR ANALYSIS

In this section we present an accurate interference analysis that considers the multipath effects on the different signals and also the timing offsets between the interfering base stations and the reference one. Direct analytical methods lead to complex integral expressions that require huge computational efforts [2]. In order to reduce the complexity of the asynchronous interference analysis, we have proposed a simpler alternative which is based on the interference power tables [4], [5].

A. Interference Tables

The interference tables model the correlation between subcarriers caused by the timing misalignment between the different transmitters (base stations in our analysis). In order to compute these tables, we refer to a reference receiver which suffers from the interference caused by an asynchronous transmitter with a timing offset τ.

1) OFDM case: Following [4], the asynchronous OFDM interference signal received on the m-th subcarrier, considering the transmission of a single complex symbol $x_{m',0}$ on the m'-th subcarrier is given by

$$y_m(\tau) = x_{m',0} e^{-j\frac{2\pi}{T}m'\tau}$$

$$\times \begin{cases} \delta(l) & \tau \in [0, \Delta] \\ e^{j\frac{\pi l}{T}(T+\tau+\Delta)} \frac{sin(\pi l(T+\Delta-\tau)/T)}{\pi l} & \tau \in [\Delta, T+\Delta] \end{cases} \tag{4}$$

where

- τ is the timing offset
- $l = m' - m$ and $\delta(l)$ is the Kronecker delta function
- T is the OFDM symbol duration
- Δ is the cyclic prefix duration

In the general case, the resulting interference power is the sum of interference powers coming respectively from two successive data symbols $(x_{m',n'-1}, x_{m',n'})$, we get then

$$I(\tau, l) =$$

$$\begin{cases} \delta(l) & \tau \in [0, \Delta] \\ \left|\frac{sin(\pi l(T+\Delta-\tau)/T)}{\pi l}\right|^2 + \left|\frac{sin(\pi l(\tau-\Delta)/T)}{\pi l}\right|^2 & \tau \in [\Delta, T+\Delta] \end{cases} \tag{5}$$

It should be noticed that the data communication symbols $x_{m',n}$ are zero mean uncorrelated variables with normalized power.

2) FBMC case: In the filter bank based system (FBMC), transmit pulses that are more localized in time-frequency domain are used [8], [18]. The orthogonality between subcarriers is maintained by introducing a half symbol period delay between the in-phase and the quadrature components of each complex symbol [18], [21]. This technique is called offset QAM (OQAM) technique.

Now, let us consider the asynchronous transmission of a sequence of real symbols $\{a_{m',n'}\}$ from the interferer to the reference user on the m'-th subcarrier

$$s_{m'}(t,\tau) =$$
$$\sum_{n'=-\infty}^{+\infty} a_{m',n'} f(t - n'T/2 - \tau) e^{j\frac{2\pi}{T}m'(t-\tau)} e^{j\varphi_{m',n'}} \tag{6}$$

where $f(t)$ is the real-valued pulse response of the prototype filter and $\varphi_{m',n'} = \frac{\pi}{2}(n' + m') - \pi n'm'$. T is the signaling interval and $1/T$ is the subcarrier spacing.

The interference signal on the m-th subcarrier of the reference receiver output can be given by (7) (see next page).

In our analysis, we refer to the PHYDYAS NPR (nearly perfect reconstruction) prototype filter using the frequency sampling technique [8]. The impulse response of this filter is defined as follows

$$f(t) =$$
$$\begin{cases} \frac{1}{\sqrt{A}} \left[1 + 2 \sum_{k=1}^{D-1} (-1)^k G_k \cos\left(\frac{2\pi}{DT}kt\right) \right] & t \in [0, DT] \\ 0 & elsewhere \end{cases}$$

where D is the overlapping factor and A is the normalization factor.

$$A = \int_0^{DT} \left[1 + 2 \sum_{k=1}^{D-1} (-1)^k G_k \cos\left(\frac{2\pi}{DT}kt\right) \right]^2 dt$$

$$= DT \left[1 + 2 \sum_{k=1}^{D-1} G_k^2 \right]$$

The parameters G_k depend on the overlapping factor D, e.g., for $D = 4$, we have $G_1 = 0.971960, G_2 = \frac{\sqrt{2}}{2}$, $G_3 = 0.235147$ and $A = 16T$ [8].

Therefore, we can rewrite (7) as follows [5]

case 1: $(-DT < (n' - n)\frac{T}{2} < \tau)$

$$y_{m,n}(\tau) = \sum_{n'=\lfloor\frac{-\tau}{T/2}\rfloor+n+1}^{2D+n-1} a_{m',n'} e^{j(\varphi_{m',n'}-\varphi_{m,n})}$$

$$\times \left. e^{-j\frac{2\pi}{T}m'\tau} \Psi(t,\tau,l) \right|_{t=\tau}^{DT+(n-n')\frac{T}{2}} \tag{8}$$

where $\lfloor\alpha\rfloor$ denotes the floor function (the largest integer less than or equal to α).

case 2: $(\tau < (n' - n)\frac{T}{2} < DT)$

$$y_{m,n}(\tau) = \sum_{n'=-2D+n+1}^{n+\lceil\frac{-\tau}{T/2}\rceil-1} a_{m',n'} e^{j(\varphi_{m',n'}-\varphi_{m,n})}$$

$$\times \left. e^{-j\frac{2\pi}{T}m'\tau} \Psi(t,\tau,l) \right|_{t=(n-n')\frac{T}{2}}^{DT+\tau} \tag{9}$$

where $\lceil\alpha\rceil$ is the ceil function (the smallest integer greater than or equal to α).

After the OQAM decision, the corresponding interference power can thus be given by the following expressions

case 1: $(-DT < (n - n')\frac{T}{2} < \tau)$

see (10) in the next page.

$$y_{m,n}(\tau) = \int\limits_{-\infty}^{+\infty} \gamma_{m,n}^*(t)s_{m'}(t,\tau)dt$$

$$= \sum_{n'=-\infty}^{+\infty} a_{m',n'}e^{j(\varphi_{m',n'}-\varphi_{m,n})}e^{-j\frac{2\pi}{T}m'\tau}\int\limits_{-\infty}^{+\infty} f(t-n'T/2-\tau)f(t-nT/2)e^{j\frac{2\pi}{T}(m'-m)t}dt \tag{7}$$

$$I(\tau,l) = \sum_{n'=\lfloor\frac{-\tau}{T/2}\rfloor+n+1}^{2D+n-1} \left| a_{m',n'}\Re\left\{ e^{j(\varphi_{m',n'}-\varphi_{m,n})}e^{-j\frac{2\pi}{T}m'\tau}\Psi(t,\tau,l)\Big|_{t=\tau}^{DT+(n-n')\frac{T}{2}}\right\}\right|^2 \tag{10}$$

$$I(\tau,l) = \sum_{n'=-2D+n+1}^{n+\lceil\frac{-\tau}{T/2}\rceil-1} \left| a_{m',n'}\Re\left\{ e^{j(\varphi_{m',n'}-\varphi_{m,n})}e^{-j\frac{2\pi}{T}m'\tau}\Psi(t,\tau,l)\Big|_{t=(n-n')\frac{T}{2}}^{DT+\tau}\right\}\right|^2 \tag{11}$$
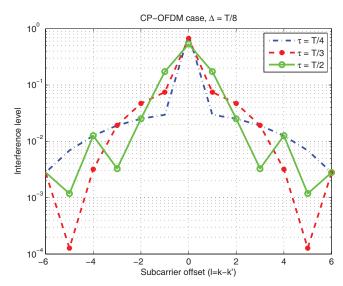

Fig. 3: The interference level in CP-OFDM for $\tau = \{\frac{T}{4}, \frac{T}{3}, \frac{T}{2}\}$.

Fig. 4: The interference level in FBMC for $\tau = \{\frac{T}{4}, \frac{T}{3}, \frac{T}{2}\}$.

case 2: $(\tau < (n-n')\frac{T}{2} < DT)$
see (11) above.

Fig. 3 and 4 show the interference power caused by different timing offsets $\tau = \{\frac{T}{4}, \frac{T}{3}, \frac{T}{2}\}$. In CP-OFDM, we have considered a CP duration of $T/8$. It is worth noting that we can model this interference power as a set of instantaneous interference tables for each timing offset τ.
Looking at Fig. 4, we observe that only immediate adjacent subcarriers are causing interference. Such a result can be explained by the better frequency localization of the PHY-DYAS prototype filter. On the other hand, Fig. 3 shows that a large number of adjacent subcarriers will cause interference (more than 8 adjacent subcarriers give an interference power greater than 10^{-3} for OFDM instead of a single one for FBMC waveform [5]). In Fig. 4, we have assumed that the overlapping factor of the prototype filter is $D = 4$.
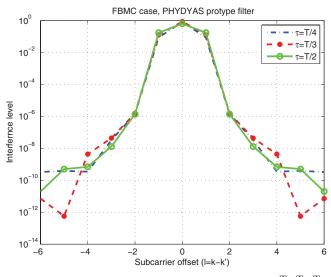
B. Interference power in a frequency selective channel

It has been demonstrated in [5], that the asynchronous interference power arriving through a frequency selective channel can be calculated using the following expression

$$P_{\text{interf}}(m,\tau) = d^{-\beta}P_{trans}(m')I(\tau,|m'-m|)\left|H(m')\right|^2 \tag{12}$$

where

- d is the distance between the interferer and the victim user
- $P_{trans}(m')$ is the transmitted power on the m'-th interfering subchannel
- $I(\tau,|m'-m|)$ is the interference table coefficient corresponding to a timing offset τ and m denotes the index of the victim subchannel
- $\left|H(m')\right|^2$ is the power channel gain between the interfering transmitter and the reference receiver on the m'-th subchannel

In the multi-cell case described in Section II, the interference is caused by the K base stations surrounding the reference cell. We can easily express the total interference power occurring at the output filter of the reference mobile user by

$$P_{\text{interf}}(m, \{\tau_k, k = 1, ..., K\}) =$$
$$\sum_{k=1}^{K} \sum_{m' \in F_k} d_k^{-\beta} P_{trans}(m') I(\tau_k, |m' - m|) |H_k(m')|^2 \quad (13)$$

F_k denotes the set of subcarriers that are assigned to the k-th base station. We recall that τ_k and $|H_k(m')|^2$ are respectively the timing offset and the power channel gain between the reference mobile user and the k-th base station.

As aforementioned, the reference mobile user is assumed to be perfectly synchronized with its base station. Consequently, the power of the desired signal can be written as

$$P_{\text{desired}}(m) = d_0^{-\beta} P_{trans}(m) |H_0(m)|^2 \quad (14)$$

In the OFDM case, it is obvious that the expression (14) is valid on the assumption that the cyclic prefix duration Δ is higher than the maximum delay spread of the channel. However in the FBMC case, the subcarrier channel gains cannot be assumed flat unless the number of subcarriers is very high. There are several approaches to deal with the frequency selective fading [18], [20], [19]. One interesting approach which is appropriate to our FBMC configuration, performs per-subcarrier equalization using finite impulse response (FIR) filters [19]. It is worth noticing that the use of multi-tap equalizers will be at the expense of a higher complexity. The purpose of this paper is to focus on the sensibility of OFDM and FBMC to the timing synchronization errors. For this reason, we assume that subcarriers experience flat fading channels.

According to (13) and (14), the SINR is given by (15), shown at the top of the next page, where N_0 denotes the noise power spectral density and B_{sc} is the bandwidth of the m-th subchannel.

IV. AVERAGE ERROR RATES ANALYSIS

The calculation of the bit error rate of any constellation is readily available in the literature when the decision variables are Gaussian random variables. [22] gives the BER of a square MQAM in AWGN channel as

$$\text{BER(SNR)} = \sum_{i=0}^{\sqrt{M}-2} \lambda_i \text{erfc} \left((2i+1) \sqrt{\frac{1}{2} \text{SNR}} \right) \quad (16)$$

where λ_is are constants that depend on the constellation size M and $\sum_{i=0}^{\sqrt{M}-2} \lambda_i = 1/2$. In the following derivation we analyze the QPSK constellation case, the extension to another MQAM constellation is straightforward.

$$\text{BER(SNR)} = \frac{1}{2} \text{erfc} \left(\sqrt{\frac{1}{2} \text{SNR}} \right) \quad (17)$$

From (15), we can rewrite the SINR in the following form,

$$\text{SINR}(m) = \frac{|H_0(m)|^2}{\sum_{k=1}^{K} \sum_{m' \in F_k} A_{k,m,m'} |H_k(m')|^2 + b} \quad (18)$$

where

$$A_{k,m,m'} = \left[\frac{d_k}{d_0} \right]^{-\beta} \frac{P_{trans}(m')}{P_{trans}(m)} I(\tau_k, |m' - m|)$$

$$b = \frac{N_0 B_{sc}}{d_0^{-\beta} P_{trans}(m)} \quad (19)$$

It should be noticed that we consider the transmitted power $P_{trans}(m)$, of each base station, as a constant. The coefficient $A_{k,m,m'}$ can thus be written as follows,

$$A_{k,m,m'} = \left[\frac{d_k}{d_0} \right]^{-\beta} I(\tau_k, |m' - m|) \quad (20)$$

Therefore, by conditioning on the set of variables $\{H_0(m), H_k(m'), \forall k, m, m'\}$ and substituting (18) in (17), we can obtain the exact closed form for the conditional error probabilities in the presence of interference (21)

$$\text{BER(SNR)}|_{H_0(m), H_k(m')} =$$
$$\frac{1}{2} \text{erfc} \left(\frac{1}{2} \frac{|H_0(m)|^2}{\sum_{k=1}^{K} \sum_{m' \in F_k} A_{k,m,m'} |H_k(m')|^2 + b} \right)^{1/2} \quad (21)$$

In order to reduce the complexity of computing the average bit error rate which requires $K \times N$ integrations into only one integration, we refer to the following lemma [17], which is based on the moment generating function of the interference power.

Lemma: Let x be a unit-mean gamma random variable (RV) with parameter α, and let y be an arbitrary non-negative random variable that is independent of x. Then

$$E_{x,y} \left[\text{erfc} \left(\frac{x}{y+b} \right)^{1/2} \right] = 1 - \frac{2}{\pi} \frac{\Gamma \left(\alpha + \frac{1}{2} \right)}{\Gamma(\alpha)}$$
$$\times \int_0^{+\infty} \frac{e^{-z}}{\sqrt{z}} {}_1F_1 \left(1 - \alpha; \frac{3}{2}; z \right) \mathcal{M}_y(\alpha z) e^{-z\alpha b} dz \quad (22)$$

where ${}_1F_1(;;)$ is the confluent hypergeometric function of the first kind [23] and $\mathcal{M}_y(z) = E_y \left[e^{-zy} \right]$ is the moment generating function (MGF) of y.

As $|H_0(m)|$ is a Rayleigh random variable, $x = |H_0(m)|^2$ is an exponential RV with a probability density function (pdf) $f(x) = e^{-x}$. In other words, x is a unit-mean gamma RV with $\alpha = 1$. Since ${}_1F_1(0; 3/2; z) = 1$, the expression (22) becomes

$$E_{x,y} \left[\text{erfc} \left(\frac{x}{y+b} \right)^{1/2} \right] = 1 - \frac{1}{\sqrt{\pi}} \int_0^{+\infty} \frac{e^{-z(1+b)}}{\sqrt{z}} \mathcal{M}_y(z) dz \quad (23)$$

A. The single interfering subcarrier case

Let us analyze the simplified case where the interference is caused only by one adjacent base station k using a single interfering subcarrier m'. We denote $|H_k(m')|^2$ by $g_{k,m'}$,

$$\text{SINR}(m) = \frac{d_0^{-\beta} P_{trans}(m) |H_0(m)|^2}{\sum\limits_{k=1}^{K} \sum\limits_{m' \in F_k} d_k^{-\beta} P_{trans}(m') I(\tau_k, |m' - m|) |H_k(m')|^2 + N_0 B_{sc}} \tag{15}$$

where $g_{k,m'}$ has the same probability density function as x. Using (21) and (23), the average error rate is given by

$$\text{BER}_{\text{average}} = \frac{1}{2} E_{x,g_{k,m'}} \left[\text{erfc} \left(\frac{1}{2} \frac{x}{A_{k,m,m'} g_{k,m'} + b} \right)^{1/2} \right]$$

$$= \frac{1}{2} - \frac{1}{2\sqrt{\pi}} \int\limits_{0}^{+\infty} \frac{e^{-z(1+2b)}}{\sqrt{z}} \mathcal{M}_{2A_{k,m,m'} g_{k,m'}}(z) dz \tag{24}$$

The MGF of $2A_{k,m,m'} g_{k,m'}$ can be calculated as follows

$$\mathcal{M}_{2A_{k,m,m'} g_{k,m'}}(z) = E_{g_{k,m'}} \left[e^{-2A_{k,m,m'} z g_{k,m'}} \right]$$

$$= \int\limits_{0}^{+\infty} e^{-2A_{k,m,m'} zt} e^{-t} dt$$

$$= \frac{1}{2A_{k,m,m'} z + 1} \tag{25}$$

Substituting (25) in (24), we obtain the final expression of the average BER for a single interfering subcarrier m' of a given base station k, which is

$$\text{BER}_{\text{average}} = \frac{1}{2} - \frac{1}{2\sqrt{\pi}} \int\limits_{0}^{+\infty} \frac{e^{-z(1+2b)}}{\sqrt{z}(2A_{k,m,m'} z + 1)} dz \tag{26}$$

In the literature [2], [6], the average error rate is computed using the mean interference power which is obtained by averaging this interference on the realizations of the interference channel gains $\{H_k(m'), m' \in F_k, k = 1, ..., K\}$. In this paper, the calculation of the average error rate has been performed by averaging the conditional BER on the all RVs including the interference channel gains.

In what follows, we study the asymptotic behavior of the average BER in (26). We mainly distinguish the interference parameter and the noise one presented respectively by $A_{k,m,m'}$ and b.

When $A_{k,m,m'} \to 0$, we have an interference-less scenario

$$\lim_{A_{k,m,m'} \to 0} \text{BER}_{\text{average}} = \frac{1}{2} - \frac{1}{2\sqrt{\pi}} \int\limits_{0}^{+\infty} \frac{e^{-z(1+2b)}}{\sqrt{z}} dz$$

$$= \frac{1}{2} - \frac{1}{2\sqrt{1+2b}} \text{erf} \sqrt{(1+2b)z} \Big|_{z=0}^{+\infty}$$

$$= \frac{1}{2} \left[1 - \frac{1}{\sqrt{1+2b}} \right] \tag{27}$$

Substituting b by $1/\text{SNR}$, we obtain

$$\lim_{A_{k,m,m'} \to 0} \text{BER}_{\text{average}} = \frac{1}{2} \left[1 - \sqrt{\frac{\text{SNR}}{\text{SNR} + 2}} \right] \tag{28}$$

This expression should be viewed as representing the best achievable performance in the presence of Rayleigh fading

[24].

In the noiseless scenario $b = 0$, the average BER is given by

$$\lim_{b \to 0} \text{BER}_{\text{average}} = \frac{1}{2} - \frac{1}{2\sqrt{\pi}} \int\limits_{0}^{+\infty} \frac{e^{-z}}{\sqrt{z}(2A_{k,m,m'} z + 1)} dz \tag{29}$$

As the interference weight $A_{k,m,m'}$ is constant, the average BER is constant for high values of SNR ($b = 1/\text{SNR}$ is negligible). Therefore, an error floor will appear because of the limitation of the system performance by the interference term.

B. The multi-cell case

The extension of this result to the multi-cell case is straightforward. In this case, the random variable related to the total interference power is defined by

$$g_{eq} = 2 \sum_{k=1}^{K} \sum_{m' \in F_k} A_{k,m,m'} g_{k,m'} \tag{30}$$

where $g_{k,m'} = |H_k(m')|^2$.

As the signals coming from the different interfering cells $\{ \sum\limits_{m' \in F_k} A_{k,m,m'} g_{k,m'}, \forall k \}$ are independent, the moment generating function of g_{eq} is given by

$$\mathcal{M}_{g_{eq}}(z) = E_{\{g_{k,m'}, \forall k, m'\}} \left[e^{-2z \sum\limits_{k=1}^{K} \sum\limits_{m' \in F_k} A_{k,m,m'} g_{k,m'}} \right]$$

$$= \prod_{k=1}^{K} E_{\{g_{k,m'}, \forall m'\}} \left[e^{-2z \sum\limits_{m' \in F_k} A_{k,m,m'} g_{k,m'}} \right] \tag{31}$$

Consequently, the MGF of g_{eq} is the product of the MGFs $\mathcal{M}_k(z)$ where

$$\mathcal{M}_k(z) = E_{\{g_{k,m'}, m' \in F_k\}} \left[e^{-2z \sum\limits_{m' \in F_k} A_{k,m,m'} g_{k,m'}} \right] \tag{32}$$

However, the RVs $\{g_{k,m'} = |H_k(m')|^2, m' \in F_k\}$ are correlated because they belong to the same cluster used by the k-th base station. To deal with this problem, let Ω_k defined by

$$\Omega_k = \left[\rho_{i,j} \right]_{(i,j) \in F_k \times F_k}$$

where $\rho_{i,j} = \rho_{j,i}$, be the square root of the variance-covariance matrix of the RVs $\{g_{k,m'}, m' \in F_k\}$.

Following [25], the MGF $\mathcal{M}_k(z)$ is obtained by

$$\mathcal{M}_k(z) = \left| I_{L_k} + 2 \Omega_k D_k^A z \right|^{-1} \tag{33}$$

where I_{L_k} is the $L_k \times L_k$ identity matrix and L_k denotes the cardinal of F_k. D_k^A is a diagonal matrix of diagonal elements,

$$D_k^A(i,i) = A_{k,m,i} \qquad i \in F_k \tag{34}$$

Substituting (33) in the expression (31), we obtain the MGF related to the total interference RV g_{eq} defined in (30),

$$\mathcal{M}_{y_{eq}}(z) = \prod_{k=1}^{K} \mathcal{M}_k(z) = \prod_{k=1}^{K} \left| I_{L_k} + 2\,\Omega_k\, D_k^A z \right|^{-1} \tag{35}$$

Therefore, using the expressions (23) and (35), the final expression of the average BER for K interfering base stations is shown in (36).

$$\mathrm{BER}_{\mathrm{average}} =$$
$$\frac{1}{2} - \frac{1}{2\sqrt{\pi}} \int_0^{+\infty} \frac{e^{-z(1+2b)}}{\sqrt{z}} \prod_{k=1}^{K} \left| I_{L_k} + 2\,\Omega_k\, D_k^A z \right|^{-1} dz \tag{36}$$

We have derived the exact expression of the average error rate in the case of block subcarrier assignment considering the frequency fading correlation between the interfering subchannels belonging to a block subcarrier of a given interfering cell.

C. The partially-loaded network

In the previous subsection, we have derived a closed-form expression of the average error rates for a fully-loaded multi-cell network. However, it is possible that a given base station may have a silent period. Consequently, the network becomes partially loaded. Let us consider a Bernoulli RV $Q_k \in (0,1)$ that models the partial load for each cell ($Q_k = 1$ when the base station k is active, and $Q_k = 0$ when it becomes inactive). We assume that $Q_k, k = 1, ..., K$ are independent with $p(Q_k = 1) = \alpha_k, \forall k$.

Our aim in this subsection is to derive a new closed-form expression of the average error rate in the partially-loaded case. The total interference RV y_{eq} can be written as follows

$$g_{eq} = 2 \sum_{k=1}^{K} Q_k A_{k,m,m'} g_{k,m'} \tag{37}$$

According to (33) and (37), the MGF $\mathcal{M}_{g_{eq}}(z)$ is expressed as follows
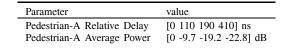
$$\mathcal{M}_{g_{eq}}(z) = \prod_{k=1}^{K} \left(1 - \alpha_k + \alpha_k \mathcal{M}_k(z)\right)$$
$$= \prod_{k=1}^{K} \left(1 - \alpha_k + \alpha_k \left| I_{L_k} + 2\,\Omega_k\, D_k^A z \right|^{-1}\right) \tag{38}$$

Therefore, using the expressions (23) and (38), the average error rate for a partially-loaded network of K interfering cells is shown in (39) (see the next page).

V. SIMULATION RESULTS

In the previous section, we have derived closed-form expressions of the average error rates in the downlink of an asynchronous K-cell network. In contrast to direct complex analytical methods, these expressions present an efficient approach to compute the average BER with a significantly

TABLE I: Channel parameters used in simulations

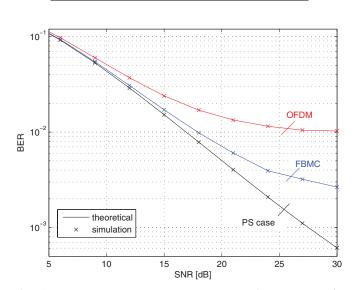| Parameter	value
Pedestrian-A Relative Delay	[0 110 190 410] ns
Pedestrian-A Average Power	[0 -9.7 -19.2 -22.8] dB

Fig. 5: The OFDM/FBMC average BER against the SNR for $\tau \in [0,T]$, the guard-band size $\delta = 0$.

reduced computational complexity. In this section, we present numerical results for the downlink of OFDM and FBMC systems with the block subcarrier scheme as described in Section II. We consider 11 interfering base stations which correspond to two tiers of the neighboring cells surrounding the reference mobile user which is located at the vertex of the cell as shown in Fig. 1. The cell radius in our simulation is R= 1km.

We have considered the Pedestrian-A model as a Rayleigh fading propagation channel where the parameters are given in Table I [27]. The choice of this model is based on the assumption that the subcarriers of interest experience flat fading channels. Therefore, we can focus on the impact of the asynchronous inter-cell interference because the intra-cell interference in the FBMC case is negligible. The path loss of a received signal at a distance d is governed by the following expression [26] corresponding to a path loss exponent $\beta = 3.76$ and a carrier frequency of 2 GHz

$$\Gamma_{loss}(d) = 128.1 + 37.6 \log_{10}(d)[dB]$$

On the other hand, we consider a system with $N = 1024$ subcarriers. The data are QPSK modulated and the sampling frequency is 10 MHz. The noise term is characterized by a thermal noise density of -174 dBm/Hz. The prefix cyclic duration is fixed at $\Delta = T/8$, and the size of the subcarrier block is set at 18 subcarriers. For the FBMC system, we recall that we use the PHYDYAS prototype filter with an overlapping factor of 4 [8]. It is worth mentioning that the following results are compared to the perfect synchronized scenario in which the orthogonality between the different subchannels is maintained.

In Fig. 5, we investigate the accuracy of the BER expres-

$$\text{BER}_{\text{average}} = \frac{1}{2} - \frac{1}{2\sqrt{\pi}} \int\limits_0^{+\infty} \frac{e^{-z(1+2b)}}{\sqrt{z}} \prod_{k=1}^{K} \left(1 - \alpha_k + \alpha_k \left| I_{L_k} + 2\,\Omega_k\, D_k^A z \right|^{-1} \right) dz \qquad (39)$$
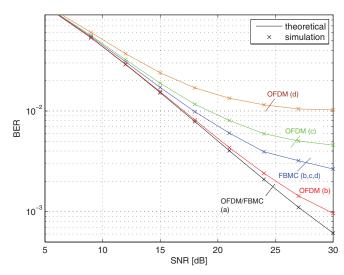

Fig. 6: The average BER for different timing offset intervals (a). PS (b). $\tau \in [0, T/7]$ (c). $\tau \in [0, T/4]$ (d). $\tau \in [0,T]$, the guard-band size $\delta = 0$.

Fig. 7: The average BER for different guard-band sizes $\delta = 0, 1, 20$, the timing offset interval $\tau \in [0,T]$.

sions corresponding to the full load case. The average BERs of OFDM and FBMC modulations are plotted against the SNR, in absence of a guard band between the clusters of the different cells ($\delta = 0$). Both theoretical and simulation results are displayed in Fig. 5. The theoretical results are evaluated using (36). The exact theoretical results depicted in Fig. 5 show an excellent match to the corresponding simulation results. In this case, we assume that the timing offset τ is a uniform RV in the interval [0,T]. Fig. 5 also shows that the timing synchronization errors cause a severe degradation in the average error rate. Moreover, this degradation becomes large when increasing the SNR level. We can also see an error floor at high SNR values. This observation can be explained by the fact that the noise level is negligible compared to the asynchronous interference caused by the other BSs. Such a case is expected in the noise-less scenario according (29). On the other hand, we observe a better performance of the asynchronous FBMC when compared to the asynchronous OFDM. Such a gain can be explained by the fact that only the two subcarriers on the edge suffer from the interference caused by their adjacent subcarriers in the FBMC case (see Fig. 4). However, in the OFDM case, the entire cluster suffers from the interference caused by all neighboring clusters (see Fig. 3). In the perfect synchronized case, both modulation schemes lead to identical results which means that the actual bit rate is higher for FBMC because it does not use CP.

In Fig. 6, we plot the average BER versus the SNR with different timing offset scenarios: the perfect synchronized case in scenario (a), [0,T/7] in scenario (b), [0,T/4] in scenario (c) and [0,T] in scenario (d).

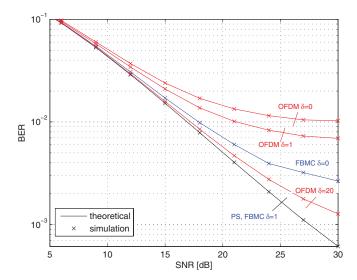In the OFDM system, the degradation is severe and in-

creases when the timing error interval is larger. We can explain this result as follows: when the timing offset is lower than the cyclic prefix duration $\tau \in [0,\Delta]$, the orthogonality between the different clusters is maintained; otherwise the reference user will suffer from an asynchronous interference. Since the timing offset is a uniform random variable, the probability obtaining the performance of the perfect synchronized case is given by the CP duration over the whole timing offset interval (Δ / τ_{max}). The probability of the orthogonality decreases as τ_{max} increases. Therefore, the average error probability becomes higher. On the other hand, the FBMC system is not sensitive to the timing offset interval length because the interference at the two subcarriers of the edge is roughly invariable with respect to the timing offset value (see Fig. 4).

The impact of the guard-band length δ on the system performance has also been investigated. Fig. 7 shows the OFDM and FBMC average BER against the SNR for different guard band values $\delta = 0, 1$ and 20 subcarriers; we assume also that the timing offset τ is a uniform RV defined on [0,T]. Comparing the different curves, one can see that the performance improves when increasing δ. However, there is still a gap with respect to the perfect synchronized case even for a guard-band of 20 subcarriers. In contrast to the OFDM case, the FBMC waveform presents an excellent performance and provides the performance of the perfect synchronized case for a guard-band of a single subcarrier $\delta = 1$. This result can also be explained by referring to Fig. 4 which shows that in FBMC, the interference power does not exceed -60 dB of the useful power when the interfering subcarrier is situated at two subcarriers from the victim one. It should be noticed that Fig. 6 and 7 show also an excellent match between the simulation
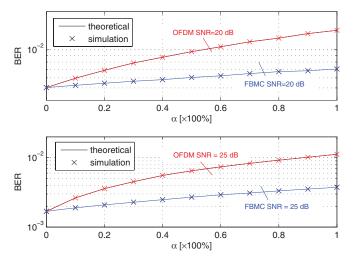
Fig. 8: The average BER against the load factor α for SNR = 20 and 25 dB, the timing offset interval $\tau \in [0,T]$.

and theoretical results obtained by the closed-form expression of the average BER given in (36).

In what follows, we analyze the system performance in a partially loaded scenario. Fig. 8 depicts the average error rates with respect to the load factor α for SNR = 20 and 25 dB, respectively. The timing offset τ is assumed uniformly distributed on [0,T]. From the results, we find that the average BER increases when increasing the load factor α. We observe also that the FBMC system still outperforms the OFDM system. Furthermore, simulation and theoretical results shown in Fig. 8 validate the accuracy of the average BER expression given in (39) for partially-loaded network.

VI. CONCLUSION

In this paper, we have investigated the impact of timing synchronization errors on the performance of the downlink of OFDM and FBMC based multi-cellular networks. We first give a brief review of the interference table model. Based on these tables, we have proposed a simpler method for the interference analysis. We then develop a theoretical derivation of the average error expressions for three scenarios: one interfering BS, several interfering BSs in a fully-loaded network and also several interfering BSs in a partially loaded network. Furthermore, the asymptotic behavior of the average error rate has been analyzed in two scenarios : the interference-less scenario and the noise-less one. Based on the interference tables and the frequency fading correlation between the interfering subchannels, we have derived the exact expression of the average error rate in the case of block subcarrier assignment. The accuracy of the obtained expressions has been validated through the different simulation results. A global evaluation has been performed taking into account different parameters: the timing error range, the guard band length and the load factor of the network. Through this evaluation, we have shown that in OFDM case, timing errors between BSs cause a severe degradation in system performance. This result is explained by the loss of orthogonality between all system subcarriers. In contrast to the OFDM system, the FBMC waveform is demonstrated to be less sensitive to timing errors between the

different cells, due to the better frequency localization of the prototype filter.

REFERENCES

[1] T. Zahariadis and D. Kazakos, "(R)evolution towards 4G mobile communication systems," *IEEE Wireless Commun. Mag.*, vol. 10, no. 4, pp. 6–7, Aug. 2003.
[2] K. A. Hamdi and Y. Shobowale, "Interference analysis in downlink OFDM considering imperfect inter-cell synchronization," *IEEE Trans. Veh. Technol.*, vol. 58, no. 7, pp. 3283–3291, Sep. 2009.
[3] R. Raghunath and A. Chockalingam, "SIR analysis and interference cancellation in uplink OFDMA with large carrier frequency and timing offsets," in *Proc. IEEE Wireless Commun. Netw. Conf.*, Mar. 2007, pp. 996-1001.
[4] Y. Medjahdi, M. Terré, D. Le Ruyet, D. Roviras, J. A. Nossek, and L. Baltar, "Inter-cell interference analysis for OFDM/FBMC systems," in *Proc. IEEE-SPAWC'09*, June 2009.
[5] Y. Medjahdi, M. Terré, D. Le Ruyet, and D. Roviras, "A new model for interference analysis in asynchronous multi-carrier transmission," submitted to *IEEE Trans. Veh. Technol.* Available: 1006.4278v1 [cs.NI].
[6] X. Wang, T. T. Tjhung, Y. Wu, and B. Caron, "SER performance evaluation and optimization of OFDM system with residual frequency and timing offsets from imperfect synchronization," *IEEE Trans. Broadcast.*, vol. 49, no. 2, pp. 170–177, June 2003.
[7] Y. Mostofi and D. Cox, "Mathematical analysis of the impact of timing synchronization errors on the performance of an OFDM system," *IEEE Trans. Commun.*, vol. 54, no. 2, Feb. 2006.
[8] M. G. Bellanger, "Specification and design of a prototype filter for filter bank based multicarrier transmission," in *Proc. IEEE Int. Conf. Acoustics, Speech, and Signal Processing*, pp. 2417–2420, May 2001.
[9] T. Pollet, M. Van Bladel, and M. Moeneclaey, "BER sensitivity of OFDM systems to carrier frequency offset and Wiener phase noise," *IEEE Trans. Commun.*, vol. 43, no. 2/3/4, pp.191–193, Feb.-Apr. 1995.
[10] T. Pollet and M. Moeneclaey, "The effect of carrier frequency offset on the performance of band limited single carrier and OFDM signals," in *Proc. IEEE GLOBECOM*, Nov. 1996, pp 719–723.
[11] T. Pollet, P. Spruyt, and M. Moeneclaey, "The BER performance of OFDM systems using non-synchronized sampling," in *Proc. IEEE GLOBECOM*, Dec. 1994, pp.253–257.
[12] J. Cheng and N. C. Beaulieu, "Accurate DS-CDMA bit-error probability calculation in Rayleigh fading," *IEEE Trans. Wireless Commun.*, vol. 1, no. 1, pp. 3–15, Jan. 2002.
[13] M. A. Landolsi and W. E. Stark, "On the accuracy of Gaussian approximations in the error analysis of DS-CDMA with OQPSK modulation," *IEEE Trans. Commun.*, vol. 50, no. 12, Dec. 2002.
[14] A. Giorgetti and M. Chiani, "Influence of fading on the Gaussian approximation for BPSK and QPSK with asynchronous cochannel interference," *IEEE Trans. Wireless Commun.*, vol. 4, no. 2, pp. 384–389, 2005.
[15] N. C. Beaulieu, "The evaluation of error probabilities for intersymbol and cochannel interference," *IEEE Trans. Commun.*, vol. 39, no. 12, pp. 1740-1749, Dec. 1991.
[16] N. C. Beaulieu, "An infinite series for the computation of the complementary probability distribution function of a sum of independent random variables and its application to the sum of Rayleigh random variables," *IEEE Trans. Commun.*, vol. 38, no. 9, pp. 1463-1474, Sep. 1990.
[17] K. A. Hamdi, "A useful technique for interference analysis in Nakagami fading," *IEEE Trans. Commun.*, vol. 55, no. 6, June 2007.
[18] P. Siohan, C. Siclet, and N. Lacaille, "Analysis and design of OFDM/OQAM systems based on filter bank theory," *IEEE Trans. Signal Process.*, vol. 50, no. 5, pp. 1170–1183, May 2002.
[19] T. Ihalainen, T. H. Stitz, M. Rinne, and M. Renfors, "Channel equalization in filter bank based multicarrier modulation for wireless communications," *EURASIP J. Adv. Signal Process.*, vol. 2007, article ID 49389, 18 pages, 2007.
[20] L. Vandendorpe, L. Cuvelier, F. Deryck, J. Louveaux, and O. van deWiel, "Fractionally spaced linear and decision-feedback detectors for transmultiplexers," *IEEE Trans. Signal Process.*, vol. 46, no. 4, pp. 996-1011, 1998.
[21] H. Boelcskei, "Orthogonal frequency division multiplexing based on offset QAM," in *Advances in Gabor Analysis*. Birkhauser, 2003.
[22] K. Cho and D. Yoon, "On the general BER expression of one and two dimensional amplitude modulation," *IEEE Trans. Commun.*, vol. 50, no. 7, pp. 1074-1080, July 2002.
[23] M. Abramowitz and I. A. Stegun, *Handbook of Mathematical Functions*. Dover, 1965.

[24] J. G. Proakis. *Digital Communications*, 4th edition. McGraw-Hill, Inc., 2001.

[25] A. S. Krishnamoorthy and M. Parthasarathy, "A multi-variate gamma-type distribution," *Annals of Mathematical Statistics*, pp. 549–557, 1951.

[26] ETSI TR 125 942, Universal Mobile Telecommunications System (UMTS); Radio Frequency (RF) system scenarios, 2010.

[27] Rec. ITU-R M.1225 1, Guidelines for evaluation of radio transmission technologies for IMT-2000, 1997.

Yahia Medjahdi was born in 1983, received the State Engineering degree from École Nationale Polytchnique of Algiers, Algeria and the M.Sc degree in signal processing for communications from the Institut Galilée, University of Paris XIII, villetaneuse, France, in 2008. He is now working toward the Ph.D. degree in CEDRIC research laboratory at Conservatoire National des Arts et Métiers (CNAM), Paris, France. His current research interests include filter banks based multicarrier systems, interference modeling and analysis in asynchronous networks and cognitive radio.

Michel Terré was born in 1964. He received the engineering degree from the Institut National des Télécommunications, Evry, France, in 1987, the Ph.D. degree in signal processing from the Conservatoire National des Arts et Métiers, Paris, France, in 1995, and the Habilitation à Diriger des Recherches (HDR) from the University Paris XIII, Villetaneuse, France in 2004. He first had an industrial career in R&D, mostly in the field of radiocommunications working successively for TRT Philips, Thalès Communications and Alcatel. He is currently professor at the Conservatoire National des Arts et Métiers, Paris. Pr. Terré is a fellow member of SEE, he was associate editor of the Annals of Telecommunications in 2008 and Technical Program Chairman of the European Wireless Conference in 2007

Didier Le Ruyet received the Eng. Degree and the Ph. D. Degree from Conservatoire National des Arts et Métiers (CNAM) in 1994 and 2001 respectively. From 1988 to 1996 he was a research engineer in the image processing and telecommunication Departments of SAGEM, France. He joined Signal and Systems Laboratory, CNAM Paris as a research assistant in 1996. From 2002 to 2009, he was an assistant professor with the Electronic and Communication Laboratory, CNAM Paris. Since 2010 he is full professor at CNAM in the CEDRIC research laboratory. He has published about 60 papers in referred journals and conferences. His main research interests lie in the areas of digital communications and signal processing including advanced channel coding, detection and estimation algorithms and multi-antenna transmission techniques for multi-user systems.

Daniel Roviras was born in 1958. He got his Engineer degree from SUPELEC in 1981. After seven years spent in industry as a Research Engineer, he joined the Electronics Laboratory of ENSEEIHT and got his Ph.D. degree from INPT in 1989. He joined the Engineering school ENSEEIHT in 1992 as an Assistant Professor and he is Full Professor since 1999. Since 2008, he is professor in Conservatoire National des Arts et Métiers in Paris where his teaching activities are related to Radio-communication systems. His research activity has been first centered around transmission systems based on infrared links. Since 1992, his topics have widened to more general communication systems as mobile and satellite communications systems, equalization and predistortion of non linear amplifiers using neural networks, multiple access methods (CDMA, LPTV, Periodic Clock Changes, FBMC,) and cooperative/cognitive radio systems. He is currently member of CEDRIC laboratory in CNAM.

Ali Dziri received the Diplôme d'Ingénieur in electrical engineering and a master in signal processing for communications from the Ecole Nationale d'Ingénieurs de Tunis (ENIT) in 1997, and 1998 respectively. In 2001, he joined the Conservatoire National des Arts et Métiers (CNAM) of Paris, where he obtained his Ph.D. in signal processing for communications in 2004. Actually, he is a Research Engineer in the CEDRIC/LAETITIA Laboratory of CNAM Paris. His research interests include statistical characterization and modeling of fading channels, performance analysis of MIMO and cooperative communications systems, video (H264 AVC, H264 SVC) and image coding, multifractal analysis.